Available online at BCREC Website: http://bcrec.undip.ac.id

Bulletin of Chemical Reaction Engineering & Catalysis, 11 (1), 2016, 27-33

Research Article

Kinetic Modeling of C_3H_6 Inhibition on NO Oxidation over Pt Catalyst

Muhammad Mufti Azis[1,2] *, Derek Creaser[2]

[1]Chemical Engineering Department, Faculty of Engineering, Gadjah Mada University, Jl. Grafika No. 2, Kampus UGM, Yogyakarta
[2]Chemical Engineering, Department of Chemistry and Chemical Engineering, Chalmers University of Technology, Göteborg, Sweden. SE-41296

Received: 10th November 2015; Revised: 1st February 2016; Accepted: 1st February 2016

Abstract

Exhaust after treatment for lean burn and diesel engine is a complex catalytic system that consists of a number of catalytic units. Pt/Al_2O_3 is often used as a model Diesel Oxidation Catalyst (DOC) that plays an important role to facilitate oxidation of NO to NO_2. In the present study, we proposed a detailed kinetic model of NO oxidation as well as low temperature C_3H_6 inhibition to simulate temperature-programmed reaction (TPR) data for NO oxidation over Pt/Al_2O_3. A steady-state microkinetic model based on Langmuir-Hinshelwood mechanism for NO oxidation was proposed. In addition, low temperature C_3H_6 inhibition was proposed as a result of site blocking as well as surface nitrite consumption. The model can explain the experimental data well over the studied temperature range.

Keywords: microkinetic modeling; DOC catalyst; NO oxidation; C_3H_6 inhibition

How to Cite: Azis, M.M., Creaser, D. (2016). Kinetic Modeling of C_3H_6 Inhibition on NO Oxidation over Pt Catalyst. *Bulletin of Chemical Reaction Engineering & Catalysis*, 11 (1): 27-33. (doi:10.9767/bcrec.11.1.412.27-33)

Permalink/DOI: http://dx.doi.org/10.9767/bcrec.11.1.412.27-33

1. Introduction

The control of emission from gasoline lean burn and diesel vehicles is a complex chemical reaction engineering process. With the implementation of stringent emission standards in several countries such as the EURO 6 standard in Europe, improvement of exhaust after treatment system is needed. The lean exhaust after treatment technology is primarily aimed at eliminating the presence of CO, hydrocarbon (HC), particulate matters (PM) and oxides of nitrogen (NO_x) in an exhaust gas outlet. For this purpose, lean exhaust after treatment consists of several units namely diesel oxidation catalyst (DOC), diesel particulate filter (DPF) and selective catalytic reduction (SCR) unit.

DOC is placed as the first catalytic unit with oxidative functionality by facilitating oxidation of HC, CO and NO. It consists of precious PGM components such as Pt and Pd which are dispersed in a high surface area washcoat support such as Al_2O_3. Oxidation of NO to NO_2 in the DOC plays an important role since NO_2 is beneficial for DPF regeneration and some SCR catalysts. In lean exhaust aftertreatment, NO oxidation reaction over Pt catalyst has been widely studied and it shows some unique char-

* Corresponding Author.
E-mail: muhammad.azis@ugm.ac.id (M.M. Azis),
Telp: +62-274-555320, Fax: +62-274-631176

acteristics. For example it is restricted by thermodynamics at high temperature, it possess hysteresis phenomenon during heating and cooling, it is structure sensitive and the reaction is inhibited by HC and CO at low temperature [1]. Recently, it has also been reported that addition of H_2 may boost the NO oxidation reaction over Pt catalysts [2, 3]. For this reason, kinetic studies of NO oxidation over Pt/Al_2O_3 have gained a lot of interests from a number of research groups. Mechanistic studies through microkinetic modeling of NO oxidation over Pt/Al_2O_3 have been widely available in literature for instance in [4-8].

Experimental studies of HC inhibition on NO oxidation has been reported in literature by using a number of HC compounds such as C_3H_6 [9, 10], C_3H_8 [11], Dodecane [11, 12] and m-xylene [12]. Among them, C_3H_6 is often used as the model HC compounds for DOC studies. The mechanism of C_3H_6 inhibition by competitive adsorption on the active sites [10] as well as C_3H_6 reaction with NO_2 to NO [9, 12] have been proposed in literature.

With a full DOC feed mixture, a number of global kinetic models are present in the literature based on the common Voltz model [13] obtained from lab tests [14, 15] to the full-scale engine rig test [16]. Recently, Khosravi *et al.* [14, 15] reported a global kinetic model for the NO oxidation reaction in the presence of C_3H_6 over Pt and bimetallic Pt:Pd catalysts which includes C_3H_6-SCR, NO oxidation, C_3H_6 oxidation and N_2O formation. In addition, the model also accounts for inhibition terms for C_3H_6 blocking as well as C_3H_6 reaction with NO_2 to NO. They exercised the C_3H_6 influence on NO oxidation by coupling the rate of NO oxidation with C_3H_6 oxidation and inserting C_3H_6 inhibition term in the denominator part of their global rate expression. To gain a deeper understanding on the reaction mechanism, some microkinetic models have also been reported in literature by including an extensive number of elementary steps to simulate a full mixture of DOC feed including the influence of HC e.g. Koop and Deutschmann [17] and Sharma and Mhadeshwar [18].

In the present study, a kinetic model to describe the mechanism of low temperature C_3H_6 inhibition on NO oxidation over Pt/Al_2O_3 was constructed. The model here was aimed to represent mechanistic features of C_3H_6 inhibition however with relatively few reaction steps. It is hoped that the model here may provide useful insights to describe a larger mechanism especially H_2 effect on NO oxidation over Pt catalyst which is part of our on going study as previously reported in [3].

2. Experimental Method

The detail of catalyst preparation and flow reactor experiments were essentially the same as described in [3]. Further, the catalyst sample had also been used in earlier study presented in [10] to ensure stable activities under the present work. Briefly repeated here, the catalyst powder of 1 wt.% Pt/Al_2O_3 was prepared by wet impregnation method. The powder was wash coated onto a cordierite monolith with the dimensions of 2 cm width and 2 cm length. The total catalyst deposited on the monolith was ca 0.5 g. For modeling purposes, Pt dispersion of 2% was used according to the CO chemisorption test in [10]. The activity measurements were conducted in a heated horizontal flow reactor. The inlet gases to the reactor were supplied from a number of mass flow controllers (Bronkhorst). Gas FTIR analyzer (MKS 2000) was used to continuously measure the outlet gases from the reactor to measure NO, NO_2, C_3H_6 in ppm level as well as H_2O in percentage level. Pretreatment steps were conducted in O_2 and H_2 flow at 450 °C, respectively.

Temperature-programmed reaction (TPR) modes were used to measure the activity of NO oxidation in the presence and absence of C_3H_6 using a heating rate of 5 °C/min. The standard inlet gases were 500 ppm NO + 8% O_2 + 0 or 200 ppm C_3H_6 + 5% H_2O in Ar balance with the total flow of 3000 mL/min (corresponds to Weight Hourly Space Velocity, WHSV, of 562 h^{-1} or equivalent to Gas Hourly Space Velocity, GHSV, of ca. 29000 h^{-1}). The TPR of NO oxidation in the absence of C_3H_6 in this paper is designated as the base case.

3. Modeling Method

The reactor is modeled as a fixed bed reactor and discretized into a number of tanks in axial direction (tanks-in-series) as displayed in Figure 1. Here, the washcoat is divided into 8 segments (tanks) based on catalyst mass where an expansion factor of 10% for each tank is used to obtain a finer discretization in the front part of monolith. To achieve reasonable computational time, we simulated 14 temperature points as follows: 120, 150, 175, 200, 210, 220, 230, 240, 250, 260, 275, 300, 325 and 350 °C. Furthermore, some assumptions were made in the present model: steady state solution was reached for each temperature; the mass transfer from gas bulk flow to the washcoat and diffusion inside washcoat were neglected; it is under ki-

netically controlled regime; the reactor operates under isothermal conditions.

In each tank k (see Figure 1), the model solved the mole balances for each species i as described in Equation (1).

$$F_{tot} \cdot (y_{i,k-1} - y_{i,k}) - \sum_j \nu_{i,j} \cdot r_{j,k} \cdot \text{Pt density} \cdot w_{s,k} = 0 \quad (1)$$

Surface components balance for each surface species w in each tank k was described by transient equation shown in Equation (2). When steady state condition is achieved, the derivative term in Equation (2) turns to zero.

$$\frac{d\theta_{w,k}}{dt} = \sum_j r_{j,k} \cdot \chi_{w,j} \quad (2)$$

Eventually, the reaction rate for each reaction step j is described according to Equations (3) and (4).

$$r_j = k_j \cdot \prod_{i=1}^{i=I} y_i^{\nu_i} \cdot \prod_{w=1}^{w=W} \theta_w^{\nu_w} \quad (3)$$

$$k_j = Ai_j \cdot \exp\left(\frac{-Ea_j}{R.T}\right) \quad (4)$$

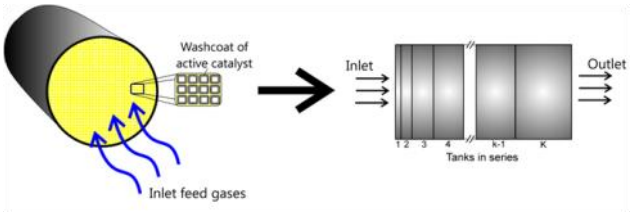

Figure 1. Reactor model used in the present study where the monolith sample was simulated with tanks in series reactor model (1D model).

All simulations were conducted with a standard personal computer and MATLAB software to solve equations (1)-(4) using ODE 15s. For parameter estimation, *lsqnonlin* function was utilized with the objective function to minimize the SSE from residuals of NO_2 and C_3H_6.

4. Results and Discussion

4.1 Rate expression and kinetic parameters

Table 1 shows the reaction mechanism used in the present model to describe NO oxidation reaction in the absence and presence of C_3H_6. As a starting point, a microkinetic model of NO oxidation based on Langmuir-Hinshelwood mechanism was used to fit the base case of NO oxidation data to yield kinetic parameters for steps 1 to 8. It should be mentioned that we do not include any coverage dependence on our rate expression to correct the activation energies (Table 1) as often presented in literature (e.g. [5, 19]).

In order to decrease the number of free parameters during the estimation procedure, some parameters were determined from literature sources. Estimation of preexponential factors and activation energies for adsorption of NO, O_2 and NO_2 (step 1,3 and 5) were extracted from literature values of Bhatia *et al.* [6]. Similarly, the preexponential factor and activation energy for surface reaction between NO^* and O^* in step 7 was also fixed to the value of Bhatia *et al.* [6]. The kinetic parameters for step 8 were estimated from thermodynamics of overall NO oxidation reaction. In addition, preexponential factors for desorption of NO (step 2), O_2 (step 4) and NO_2 (step 6) were fixed at 1013 s^{-1}.

The influence of C_3H_6 on NO oxidation reaction is shown in step 9 to 12. To keep the model to be relatively simple and focused on the C_3H_6 inhibition effect on NO oxidation, other reac-

Table 1. Reaction mechanism and reaction rates used in the present model (both preexponential factors and activation energies were estimated from thermodynamics of overall NO oxidation)

Forward Reaction Rate (s^{-1})	Reaction Steps	Backward Reaction Rate (s^{-1})
$r_1 = k_1.y_{NO(g)}.\theta_v$	$NO_{(g)} + * \Leftrightarrow NO^*$ (5)	$r_2 = k_2.\theta_{NO}$
$r_3 = k_3.y_{O2(g)}.\theta_v^2$	$O_{2\,(g)} + 2* \Leftrightarrow 2O^*$ (6)	$r_4 = k_4.\theta_O^2$
$r_5 = k_5.y_{NO2(g)}.\theta_v$	$NO_{2\,(g)} + * \Leftrightarrow NO_2^*$ (7)	$r_6 = k_6.\theta_{NO2}$
$r_7 = k_7.\theta_{NO}.\theta_O$	$NO^* + O^* \Leftrightarrow NO_2* + *$ (8)	$r_{8^a} = k_8.\theta_{NO2}.\theta_v$
$r_9 = k_9.y_{C3H6(g)}.\theta_v^2$	$C_3H_{6\,(g)} + 2* \Leftrightarrow {}^*C_3H_6^*$ (9)	$r_{10} = k_6.\theta_{C3H6}$
$r_{11} = k_{11}.\theta_{C3H6}.\theta_O$	${}^*C_3H_6^* + 9O^* \Longrightarrow 3CO_2 + 3H_2O + 11*$ (10)	-
$r_{12} = k_{12}.\theta_{C3H6}.\theta_{NO2}$	${}^*C_3H_6^* + 9NO_2^* \Longrightarrow 9\,NO + 3CO_2 + 3H_2O + 11*$ (11)	-

tions such as C_3H_6-SCR and N_2O formation steps were not included in the present model. Adsorption of C_3H_6 (step 9) was assumed to occupy 2 vacant sites which resembles the O_2 adsorption step. The inhibition effects by blocking (step 9) as well as irreversible surface reaction between $C_3H_6^*$ with NO_2^* (step 12) were included to represent C_3H_6 inhibition steps. In addition, irreversible C_3H_6 oxidation reaction (step 11) was included to represent combustion of C_3H_6.

The preexponential factor for C_3H_6 desorption (step 10), C_3H_6 oxidation (step 11) and C_3H_6 surface reaction with NO_2^* (step 12) were fixed at 1013 s^{-1}. Additionally, the activation energy of C_3H_6 adsorption (step 9) was assumed to be 0 kJ/mol showing a non-activated adsorption process. Eventually, one preexponential factor (step 9) and 6 activation energies (steps 2, 4, 6, 10, 11, and 12) were optimized from non-linear regression. Table 2 presents the final list of kinetic parameters used in the present model.

4.2. Temperature-programmed reaction of NO oxidation (base case)

Comparison between simulation and experimental TPR data of NO oxidation base case is presented in Figure 2. The activity measurement here only present the data up to 350 °C as NO oxidation reaction is commonly restricted by thermodynamics beyond this temperature as shown by the equilibrium line in Figure 2. As shown from the top panel of Figure 2, an excellent agreement was achieved through simulation of 14 experimental data within the studied temperature interval.

From the lower panel of Figure 2, the variation of surface species coverages as a function of temperature is presented. As seen here, NO^* is the predominant species at low temperature as in agreement with the model of Bhatia *et al.* [6]. By increasing temperature, it is apparent that NO oxidation reaction progressed more rapidly which gave higher coverage of NO_2^*. Eventually, further increase in temperature caused the increase in O^* coverage which is conceivable as the activation energy for O^* is the highest among all steps (reaction 4). In addition, high coverage of O^* at high temperature as presented here confirmed the presence of Pt-Oxide formation which is known over Pt catalyst. Pt oxide formation itself is known to cause deactivation and hysteresis effect on NO oxidation reaction as reported in [6, 20-22].

4.3. Modeling C_3H_6 inhibition on NO oxidation

The inhibition effect from the presence of minute concentrations of C_3H_6 on NO oxidation has been widely reported in literature as confirmed by the results presented in Figure 3.

Table 2. The list of kinetic parameters used in the present model

Step	A_i (s^{-1})			E_a (kJ/mol)		
1	1.875×10^8	fixed	ref [6][a]	0	fixed	ref [6]
2	1×10^{13}	fixed		73.93	estimated	
3	1.175×10^7	fixed	ref [6] [a]	30.4	fixed	ref [6]
4	1×10^{13}	fixed		150.56	estimated	
5	2.00×10^8	fixed	ref [6] [a]	0	fixed	ref [6]
6	1×10^{13}	fixed		91.35	estimated	
7	1.125×10^{13}	fixed	ref [6] [a]	101.3	fixed	ref [6]
8	1.0177×10^{14}	constrained		116.66	constrained	
9	4.36×10^8	estimated		0	fixed	
10	1×10^{13}	fixed		99.03	estimated	
11	1×10^{13}	fixed		146.82	estimated	
12	1×10^{13}	fixed		46.54	estimated	

[a] To obtain the same unit of preexponential factors as in ref. [6], the preexponential factors presented here need to be multiplied by 40 mol Pt/m^3 washcoat [8].

Strong inhibition of C_3H_6 at low temperature is generally observed up to a temperature point where full conversion of C_3H_6 is achieved (at ca. 220 °C).

Comparison between simulation and experimental data is also shown in Figure 3. The result from steady state modeling from 14 experimental data gave an excellent agreement with experimental data. With the aid of the lower panel in Figure 3, mean surface coverages of various species is presented as a function of temperature. As expected at low temperature, the predominant surface species is $C_3H_6^*$ that blocks the active sites. As the temperature increases, the mean coverage of $C_3H_6^*$ decreases and O^* appears as the dominant species on the catalyst. The increase of NO_2 outlet concentration (upper panel Figure 3) appears to be in parallel with the increase of O^* which suggested that O^* plays crucial role in the NO oxidation reaction. Comparing the NO_2 yield above 220 °C where all C_3H_6 has been fully converted, it can be seen that the NO_2 yield in the presence of C_3H_6 (Figure 3) is lower than the NO_2 yield from the base case (Figure 2). Hence, it is likely that C_3H_6 plays a role to decrease the NO_2 yield. For this reason, the present model includes reaction 12 to illustrate the role of $C_3H_6^*$ to lower the NO_2 yield by reducing NO_2^* (surface nitrite) and it turns out that kinetic parameters for this reaction were sensitive to influence the profile of C_3H_6 and NO_2.

Further evaluation can also be made to analyze the axial profile of NO_2 gas concentration inside the monolith washcoat as shown in Figure 4. Below the light-off temperature for NO oxidation, the coverage of $C_3H_6^*$ suppresses the NO_2 yield in the entire monolith. When the temperature increases, the reaction front for NO oxidation initiated from the rear part of monolith. As the temperature increases, production of NO_2 propagates to-

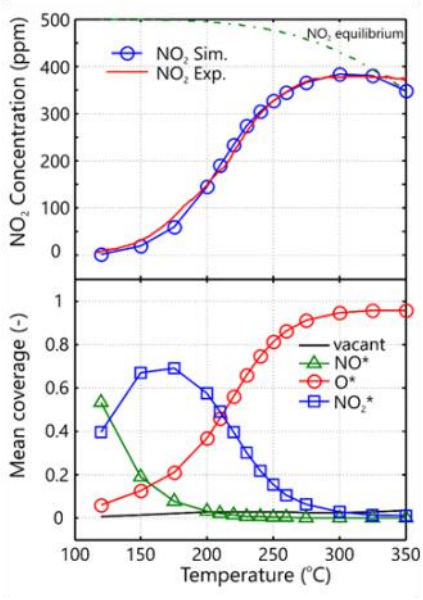

Figure 2. Comparison between simulation and experimental results from TPR of NO oxidation (*base case*) over 1 wt.% Pt/Al_2O_3 catalyst: gas concentrations (top panel) and surface species coverages (bottom panel). The inlet feed conditions: 500 ppm NO, 8% O_2, 5% H_2O with Ar balance.

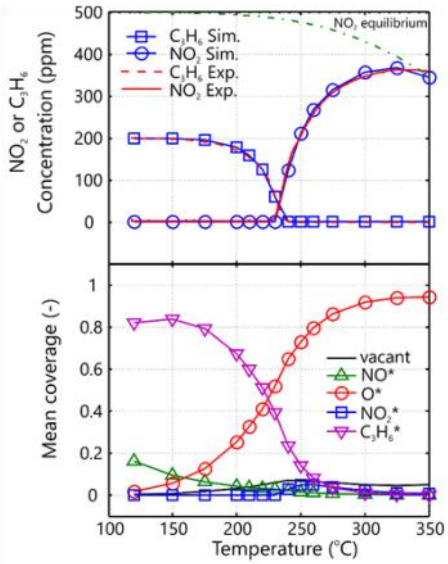

Figure 3. Comparison between simulation and experimental results from TPR of NO oxidation in the presence of C_3H_6 over 1 wt.% Pt/Al_2O_3 catalyst: gas concentrations (top panel) and surface species coverages (bottom panel). The inlet feed conditions: 500 ppm NO, 200 ppm C_3H_6, 8% O_2, 5% H_2O with Ar balance.

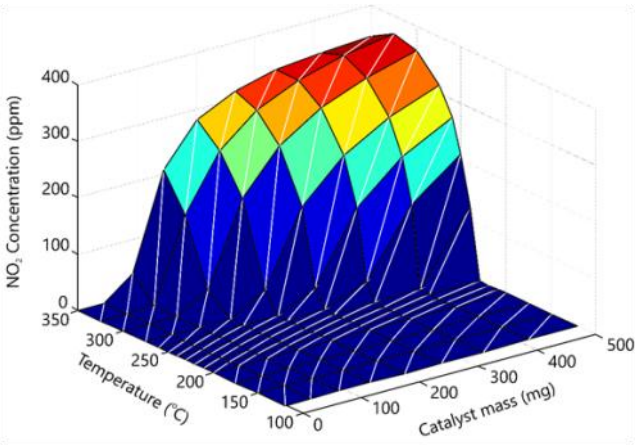

Figure 4. Model prediction for axial distribution of NO_2 in the monolith Pt/Al_2O_3 catalyst for various temperatures. The inlet feed condition is the same as in Figure 3.

wards the front part of monolith. As a result, a larger part of the washcoat is utilized for production of NO_2 in parallel with the increase of temperature.

5. Conclusions

An inhibition effect due to addition of C_3H_6 has a substantial influence on NO oxidation reaction over Pt/Al_2O_3 catalyst. A detailed kinetic model for NO oxidation (base case) has been constructed based on Langmuir-Hinshelwood mechanism using TPR data. The NO oxidation model was then extended to include inhibition effects due to addition of C_3H_6 on NO oxidation. Two mechanisms of C_3H_6 inhibition were included in the model: site blocking as well as surface nitrite consumption. The simulations show that the proposed model based on 7 fitted kinetic parameters can capture the experimental data well over the studied temperature range for both the base case and NO oxidation in the presence of C_3H_6.

Acknowledgments

The financial support by the Swedish Research Council with grant number 621-2011-3926 is gratefully acknowledged. MMA would also like to thank *Program Hibah Publikasi* from UGM to support the publication of this work. This work was performed within the Competence Centre for Catalysis, which is hosted by Chalmers University of Technology and financially supported by the Swedish Energy Agency and the member companies AB Volvo, ECAPS AB, Haldor Topsøe A/S, Scania CV AB, Volvo Car Corporation AB and Wärtsilä Finland Oy. MMA would also like to acknowledge Dr. Xavier Auvray for collaborative experimental work performed in this study.

Nomenclatures

Roman symbols

A_i: preexponential factors (s^{-1})
E_a: activation energy ($kJ.mol^{-1}$)
F_{tot}: molar flow rate ($mol.s^{-1}$)
K: rate constant (s^{-1})
Pt density: Pt site density ($mol.kg^{-1}$)
r: reaction rate (s^{-1})
R: gas constant ($J.mol^{-1}.K^{-1}$)
T: temperature (K)
t: time step (s)
w_s: mass of segmental catalyst (kg)
y: molar fraction (-)

Greek symbols

θ: fractional surface coverage (-)
ν: stoichiometric coefficient (-)
χ: stoichiometric coefficient of adsorbed species (-)

Subscript

i: gas component index
j: reaction index
k: tank index
w: surface component index

References

[1] Russell, A., Epling, W.S. (2011). Diesel Oxidation Catalysts. *Catalysis Reviews*, 53: 337-423.

[2] Herreros, J.M., Gill, S.S., Lefort, I., Tsolakis, A., Millington, P., Moss, E. (2014). Enhancing the low temperature oxidation performance over a Pt and a Pt-Pd diesel oxidation catalyst. *Applied Catalysis B: Environmental*, 147: 835-841.

[3] Azis, M.M., Auvray, X., Olsson, L., Creaser, D. (2015). Evaluation of H_2 effect on NO oxidation over a diesel oxidation catalyst. *Applied Catalysis B: Environmental*, 179: 542-550.

[4] Olsson, L., Westerberg, B., Persson, H., Fridell, E., Skoglundh, M., Andersson, B. (1999). A Kinetic Study of Oxygen Adsorption/Desorption and NO Oxidation over Pt/Al_2O_3 Catalysts. *The Journal of Physical Chemistry B*, 103: 10433-10439.

[5] Olsson, L., Persson, H., Fridell, E., Skoglundh, M., Andersson, B. (2001) A Kinetic Study of NO Oxidation and NO_x Storage on Pt/Al_2O_3 and $Pt/BaO/Al_2O_3$. *The Journal of Physical Chemistry B*, 105: 6895-6906.

[6] Bhatia, D., McCabe, R.W., Harold, M.P., Balakotaiah, V. (2009) Experimental and kinetic study of NO oxidation on model Pt catalysts. *Journal of Catalysis*, 266: 106-119.

[7] Hauptmann,W., Votsmeier, M., Gieshoff, J., Drochner, A., Vogel, H. (2009) Inverse hysteresis during the NO oxidation on Pt under lean conditions. *Applied Catalysis B: Environmental*, 93: 22-29.

[8] Xu, J., Harold, M.P., Balakotaiah, V. (2009) Microkinetic modeling of steady-state $NO/H_2/O_2$ on $Pt/BaO/Al_2O_3$ NO_x storage and reduction monolith catalysts. *Applied Catalysis B: Environmental,* 89: 73-86.

[9] Irani, K., Epling, W.S., Blint, R. (2009) Effect of hydrocarbon species on no oxidation over diesel oxidation catalysts. *Applied Catalysis B: Environmental*, 92: 422-428.

[10] Auvray, X., Olsson, L. (2015) Stability and activity of Pd-, Pt- and Pd–Pt catalysts supported on alumina for NO oxidation. *Applied Catalysis B: Environmental*, 168-169: 342-352.

[11] Olsson, L., Abul-Milh, M., Karlsson, H., Jobson, E., Thormählen, P., Hinz, A. (2004) The effect of a changing lean gas composition on the ability of NO_2 formation and NOx reduction over supported Pt catalysts. *Topics in Catalysis*, 30-31: 85-90.

[12] Al-Harbi, M., Hayes, R., Votsmeier, M., Epling, W.S. (2012) Competitive NO, CO and hydrocarbon oxidation reactions over a diesel oxidation catalyst. *The Canadian Journal of Chemical Engineering*, 90: 1527-1538.

[13] Voltz, S.E., Morgan, C.R., Liederman, D., Jacob, S.M. (1973) Kinetic Study of Carbon Monoxide and Propylene Oxidation on Platinum Catalysts. *Product R&D*, 12: 294-301.

[14] Khosravi, M., Abedi, A., Hayes, R.E., Epling, W.S., Votsmeier, M. (2014) Kinetic modelling of Pt and Pt:Pd diesel oxidation catalysts. *Applied Catalysis B: Environmental*, 154-155: 16-26.

[15] Khosravi, M., Sola, C., Abedi, A., Hayes, R.E., Epling, W.S., Votsmeier, M. (2014) Oxidation and selective catalytic reduction of NO by propene over Pt and Pt:Pd diesel oxidation catalysts. *Applied Catalysis B: Environmental*, 147: 264-274.

[16] Lundberg, B., Sjöblom, J., Johansson, Å., Westerberg, B., Creaser, D. (2014) Parameter Estimation of a DOC from Engine Rig Experiments with a Discretized Catalyst Washcoat Model. *SAE Int. J. Engines*, 7: 1093-1112.

[17] Koop, J., Deutschmann, O. (2009) Detailed surface reaction mechanism for Pt-catalyzed abatement of automotive exhaust gases, *Applied Catalysis B: Environmental*. 91: 47-58.

[18] Sharma, H., Mhadeshwar, A. (2012) A detailed microkinetic model for diesel engine emissions oxidation on platinum based diesel oxidation catalysts (DOC). *Applied Catalysis B: Environmental*, 127: 190-204.

[19] Crocoll, M., Kureti, S., Weisweiler, W. (2005) Mean field modeling of NO oxidation over Pt/Al_2O_3 catalyst under oxygen-rich conditions. *Journal of Catalysis*, 229: 480-489.

[20] Olsson, L., Fridell, E. (2002) The Influence of Pt Oxide Formation and Pt Dispersion on the Reactions $NO_2 \Leftrightarrow NO+1/2O_2$ over Pt/Al_2O_3 and $Pt/BaO/Al_2O_3$. *Journal of Catalysis*, 210: 340-353.

[21] Hauff, K., Tuttlies, U., Eigenberger, G., Nieken, U. (2012) Platinum oxide formation and reduction during NO oxidation on a diesel oxidation catalyst - Experimental results. *Applied Catalysis B: Environmental*, 123-124: 107-116.

[22] Hauff, K., Dubbe, H., Tuttlies, U., Eigenberger, G., Nieken, U. (2013) Platinum oxide formation and reduction during NO oxidation on a diesel oxidation catalyst-Macrokinetic simulation. *Applied Catalysis B: Environmental*, 129: 273-281.

Selected and Revised Papers from The 2nd International Conference on Chemical and Material Engineering 2015 (ICCME 2015) (29-20 September, 2015, Semarang, Indonesia) (http://econference.undip.ac.id/index.php/iccme/2015) after Peer-reviewed by ICCME 2015 and BCREC Reviewers